Journal of Polymer Research (2022) 29:521
https://doi.org/10.1007/s10965-022-03375-x

ORIGINAL PAPER

Synthesis and properties of bio-based thermoplastic poly(ether urethane) for soft actuators

Yang Sook Jung[1] · Jeongjae Woo[1] · Eunsol Lee[1] · Sunhee Lee[2] · Eun Joo Shin[1]

Received: 24 August 2022 / Accepted: 16 November 2022 / Published online: 24 November 2022

Abstract

In this study, bio-based thermoplastic polyurethane (TPU) for use in soft actuators is bio-based poly(ether-urethane) made using fermented corn, along with bio-derived compounds such as propane-1,3-diol (PDO) as a chain extender. Bio-based TPUs were obtained through a solvent-free one-shot synthesis method, and the effects of varying the [NCO]/[OH] molar ratio and type of isocyanates on chemical structure, thermal stability, and mechanical properties were investigated. The degree of phase separation (DPS) and state of hard segment (HS) / soft segment (SS) of TPU are important factors affecting the thermal and physical properties of the prepared film. These properties depend on the [NCO]/[OH] molar ratio and the type of isocyanates used for polymerization. The results showed that, when aromatic isocyanate was used, the degree of separation of the HS/SS was improved as the molar ratio increased. The average molecular weight and DPS as well as thermal and mechanical properties of 1-isocyanato-4-[(4-isocyanatophenyl)methyl]benzene (MDI)-based TPU samples are all higher than those of 1,1'-methylenebis(4-isocyanatocyclohexane) (H_{12}MDI)-based TPU samples in spite of the lower HS content. These findings of this study are expected to contribute to the preparation of fused deposition modeling (FDM) 3D printing or 4D printing for shape memory polymer from bio-based TPU filaments for use in soft actuators with a shore hardness range of 59~84A.

Keywords Thermoplastic polyurethane (TPU) · Bio-based · Isocyanate · Polyol · Polyether · Chain extender

Introduction

One type of polyurethane material that has recently been attracting increased interest is thermoplastic polyurethane. Thermoplastic polyurethanes (TPUs) are unique polymeric materials with a wide range of physical and chemical properties. They are applied in various industrial fields, such as in synthetic rubbers, foams, fibers, elastomers, protective coating, biomaterials, membranes, rigid devise, sealants, and adhesives [1–4].

✉ Sunhee Lee
shlee014@dau.ac.kr

✉ Eun Joo Shin
sejoo6313@dau.ac.kr

Yang Sook Jung
9jungys@gmail.com

[1] Department of Organic Materials and Polymer Engineering, Dong-A University, 37 Nakdong-daero 550beon-gil, Saha-gu, 49315 Busan, Republic of Korea

[2] Department of Fashion Design, Dong-A University, 37 Nakdong-daero 550beon-Gil, Saha-gu, 49315 Busan, Republic of Korea

TPUs have conventionally been prepared from a dihydroxyl-terminated precursor (polymer diol), an isocyanate, and a chain extender. These materials are characterized by a segmented structure that is formed by two types of segments: flexible and soft segments (SS) consisting of polyols (polyester or polyether diols) and hard segments (HS) composed of products of the reaction of isocyanates and chain extenders [5, 6]. The isocyanate, a component of the hard segment, has two NCO groups capable of reacting with polyols, chain extenders, and crosslinking agents [7, 8]. However, even for isocyanate compounds with the same NCO, each compound has a different molecular shape and different properties; therefore, different compounds are best applied in different fields. Both aliphatic and aromatic isocyanates can be used to synthesize TPU [9]. The two most used aromatic isocyanates in TPU synthesis are 2,4-diisocyanato-1-methylbenzene (TDI) and 1-isocyanato-4-[(4-isocyanatophenyl) methyl] benzene (MDI). Although TDI is less expensive than MDI, MDI has superior reactivity and polymers based on MDI may possess good physical properties. The typical aliphatic isocyanates include 1,6-diisocyanatohexane (HDI), 5-isocyanato-1-(isocyanatomethyl)-1,3,3-trimethylcyclohexane (IPDI), and 1,1'-methylenebis(4-isocyanatocyclohexane)

(H_{12}MDI) [10]. The choice of chain extender and isocyanate determines the characteristics of HS, and to a large extent, the physical properties of a TPU. The most important chain extenders for TPU are linear glycols such as propane-1,3-diol (PDO) and butane-1,4-diol (BDO). The polyols typically used to prepare TPUs are dihydroxyl-terminated amorphous and semicrystalline polymers with a molecular weight ranging from 600 to 4000 g/mol [11], preferably from 1000 to 2000 g/mol. In general, polyols available for TPU synthesis include polyesters, polyethers, polysiloxanes, polycarbonates, polyolefins, or mixtures of two or more of these. TPU synthesized from polyesters possess relatively high physical property level, especially with respect to elasticity, tensile strength, and initial modulus [9]. This property can also be disadvantageous, because of the hardening or decrease upon elongation. Polyether-based TPU exhibit to lower of viscosity of polyurethane composition leading to softening, which is beneficial during industrial processing [12]. Polyether-based polyol is more suitable in TPU synthesis for soft actuators. And the ether-base polyols—such as poly(ethane-1,2-diol) and poly (tetra methylene -1,2-diol)—possess better hydrolytic stability than poly(ester urethane)s, in which the SSs undergo fast hydrolysis [13]. However, these are susceptible to oxidative degradation, which results in chain scission and crosslinking. The melting point is higher as the polyether polyol chain length increases [14, 15].

TPUs are traditionally prepared through various synthesis methods with different preparation media (solvent–free, in solution, in water) according to the sequence in which the reactants are added (one–shot process, pre–polymer process) [16]. In the pre–polymer process, polyols and isocyanates first react to form an isocyanate-terminated pre–polymer, which is followed by the second step of chain extension wherein the chain extender is added. Numerous TPU elastomers are prepared using NCO pre–polymer intermediates. This method allows for the complete reaction of even low reactivity polyether diols in the absence of catalysts and allows for the intentional preparation of a segmented structure. In the one-shot process, all the starting materials are mixed in one reactor, and polymerization is performed. This process which is carried out without the use of solvents is typically very fast, specifically in the presence of catalysts. Therefore, materials formed utilizing the one-shot process are prepared by simultaneously mixing all the coreactants directly with the additives [17]. The reaction is very exothermic and, depending on the catalysis applied, is substantially terminated within 2 to 30 min.

However, the growing demand for plastics, including TPUs, is associated with serious environmental pollution. Specifically, the synthesis and application of TPUs with many volatile organic compounds (VOCs) such as isocyanates, polyols, catalysts, additives, and so on, emit hazardous pollutants that cause serious environmental pollution. The chemical industry is therefore researching new solutions that are based on raw materials of natural origin. A new trend is to replace petrochemical polyols and chain extenders used in the synthesis of TPUs with materials obtained from biomass, including polysaccharides, sugars (e.g., xylose, mannose, glucose, galactose, idose, etc.), lignin, and vegetable oils (such as soybean oil, castor oil, rubber seed oil and palm oil) [18–21]. Biocompatible polyols with their non-toxic, biodegradable, and eco-friendly advantages are gaining extensive research attention. Recently there are many works available at the literature describing selected application of the bio-based TPUs obtained with using bio-based polyol and examples were described below. Miao et al. [22, 23] reviewed the recent developments in the synthesis of seed oil-based TPUs and applications in the biomedical devices. Shin et al. [24] investigated a soft-actuator grade thermoplastic polyurethane (TPU) with 73–86 shore A with the use of bio-based polyol. And Wehner et al. [25] developed soft robots by the combined fabrication techniques, with the body via molding, microfluidic logic via soft lithography, and the pneumatic actuator networks, embedded 3D printing technique to obtain completely soft, autonomous robots. Petrovic et al. [26] and many other scientists [27–30] investigated novel bio-based shape memory TPU for 3D printing. This study is focused on green thermoplastic polyurethanes (TPU) obtained using bio-based polyol and chain extender. Therefore, TPU for soft actuators was synthesized using PO3G (Poly trimethylene Ether Glycol, SK Chemical), a bio-polyol made with fermented corn. PO3G is a 100% bio-based polyether polyol that can replace existing petro–based polyols. It possesses hydroxyl group in a linear polymer chain that can directly react with isocyanates to produce TPUs, and excellent biodegradability as well as thermal and oxidation stability [31]. Meanwhile, the application of conventional organic solvent–based TPUs also involves the emission of VOCs. In response to the increasing awareness of environmental protection, we synthesized solvent-free bio-based TPUs through one-shot polymerization. One-shot synthesis methods are more commonly used in industrial applications. The solvent-free and one-shot synthesis of bio-based TPUs has considerable theoretical and practical value.

In this study, bio–based TPUs were synthesized and investigated in terms of their compositions, molecular weights, and thermal and mechanical properties. Specifically, we studied how the chemical composition (e.g., the types of HS, lengths of HS, HS contents, etc.) differs according to the type of isocyanate (MDI; Aromatic diisocyanate, H_{12}MDI; Aliphatic diisocyanate), and the molar ratio [NCO]/[OH] groups [32–36]. The [NCO]/[OH] is controlled by the main ingredients used and their contents: isocyanates, chain extenders, and polyols. In this study, TPUs with different [NCO]/[OH] ratios are typically synthesized by changing

the amount of isocyanate while keeping the contents of other components constant. The [NCO]/[OH] ratio and the type of isocyanate both strongly influence the phase separation tendencies between hard and soft segments of TPU that are closely correlated with their properties.

Experimental

Materials

We prepared TPUs with different segments by varying the molar structure and the molar mass of the HS. The HS consists of 1-isocyanato-4-[(4-isocyanatophenyl)methyl]benzene (MDI), 1,1'-methylenebis(4-isocyanatocyclohexane) (H_{12}MDI), and bio-based propane-1,3-diol (PDO) as the chain extender, all of which were obtained from Sigma Aldrich. The used bio-based polyol (Polytrimethylene ether glycol), PO3G (ecoprol 2000, SK chemical), was a gift from SK (Korea). It is produced by a corn sugar and has a bio content of 100% with the average molar mass (M_n) of 1000 g/mol, hydroxyl number 102.0–124.7 mg KOH/g, T_m 12–14 °C, and moisture max. 200 ppm. Dibutyltin dilaurate (DBTDL) was purchased from Sigma Aldrich and used as a catalyst. All materials were used after moisture removal process as received without further purification.

Sample preparation

TPUs were synthesized using a solvent-free one-shot polymerization procedure. The molar ratios of the NCO groups of MDI or H_{12}MDI to the OH groups of polyol and PDO were maintained at 1:2:1, 1:2.5:1, and 1:3:1, and the resulting TPUs were identified as presented in Table 1. The frozen MDI was melted in the oven at 80 °C for 4 h. In the one-shot method, the PO3G polyols ($M_n = 1000$) and the chain extender PDO were thoroughly mixed in polypropylene beakers using a mechanical stirrer, then placed in an oven with the temperature maintained at 80 °C. Next, diisocyanate H_{12}MDI or MDI and catalyst DBTDL(0.03wt%) were added to the reaction mixture and mechanically stirred at room temperature for 1–2 min. As the mixture was stirred and polymerized, the transparent liquid mixture became opaque, and then TPU was obtained. The reaction mixture was poured into a Teflon-coated pan and cured in an oven at 100 °C for 24 h and kept to complete polymerization. The final product was pressed at 180 °C for 5 min to obtain the film. After being allowed to cool to room temperature, the 1–2 mm thick sheet was taken out from the mold and used for further structural, thermal, and mechanical analyses and characterizations.

Table 1 Formulation design of bio-based TPUs samples

Sample	Diisocyanate	OH/NCO/OH	HS content (wt%)[a]	Content of bio-based sources (wt%)[b]
HP-2.0	H_{12}MDI	1:2.0:1	37.1	63
HP-2.5	H_{12}MDI	1:2.5:1	41.8	58
HP-3.0	H_{12}MDI	1:3.0:1	46.0	54
MP-2.0	MDI	1:2.0:1	37.1	63
MP-2.5	MDI	1:2.5:1	41.6	58
MP-3.0	MDI	1:3.0:1	45.7	54

[a] Hard segment concentration is defined as the ratio of the mass of non-polyol components to the total mass of the polymer

[b] Bio-content is defined as the ratio of the mass of bio-based components to the total mass of the polymer

Measurements

Structure characterizations

Weight-average molecular weight (Mw), average molar mass (Mn), and polydispersity index (PDI) were measured by gel permeation chromatography (GPC) using a Viscotek GPCmax VE-2001. THF was used as a mobile phase solvent at a flow rate of 1 mL min^{-1} at 60 °C. The column was 300 × 810 mm. Fourier transform infrared spectroscopy (FT-IR) measurements were performed using a Nicolet Nexus FT-IR spectrometer (Perkinelmer, UK) over the range $400 - 4000\ cm^{-1}$ equipped with an attenuated total reflectance accessory (ATR).

Thermal characterizations

Differential Scanning Calorimetry (DSC) was conducted on a thermal analyzer DSC 8500 analyzer (TA Instrument, USA). All the samples were weighted between 2 and 10 mg. The measurements were carried out in a heating–cooling-heating cycle from –70 °C to 250 °C where the heating rate was 20 °C/min under a nitrogen purge. Dynamical mechanical thermal analysis (DMA) of the TPU films was performed on a DMA Q800 analyzer (TA instruments, USA) in the tensile mode at the frequency of 1 Hz. The samples were first cooled to – 100 °C before being heated to 150 °C at a rate of 4 °C/min.

Thermogravimetric analysis (TGA) was conducted using TGA Q500 (TA Instrument, USA), which was run at a temperature range from 40 °C to 650 °C with a ramp heating rate of 10 °C/min in the presence of nitrogen atmosphere. The weight of each sample was ca. 5 mg. The weight losses of 5% and 50% as well as maximum degradation rate and ash residue at 600 °C were registered.

Table 2 Average molecular weight (M_n/ M_w) and polydispersity index (PDI) of bio-based TPUs

Sample	M_n	M_w	PDI
HP-2.0	26,796	44,160	1.65
HP-2.5	28,664	51,310	1.79
HP-3.0	31,802	53,859	1.69
MP-2.0	27,115	44,521	1.64
MP-2.5	33,655	60,114	1.79
MP-3.0	32,996	60,141	1.82

Mechanical characterizations

Shore A hardness was measured at room temperature using a Zwick Roell GS-706 N(TECLOCK, Japan) analogical hardness testing apparatus following the UNE-EN ISO 868:1998: Plastics and ebonite. Determination of indentation hardness by means of a durometer (Shore hardness) standard procedure at (23 ± 2) °C and 50% relative humidity. Mechanical properties of the TPUs films were obtained using an autograph tester from Instron 4201 (Simadzu, Japan) to measure the stress–strain behavior of the samples with tension.

Results and discussions

Average molecular weight

The M_n, M_w, and PDI of the TPUs were determined by GPC analysis, and the relevant data are summarized in Table 2. The M_n and M_w of TPUs were in the respective ranges of 26,796–32,996, and 44,160–60,141. The M_w of TPUs increased substantially with increasing [NCO]/[OH] molar ratio. As the [NCO]/[OH] molar ratio increases, the number of urethane units contained in hard domains increases as well, thus resulting in a higher molecular weight [36, 37]. The MP-series have higher molecular weights than the HP-series despite having similar hard segment mole ratios, as presented in Table 2.

The PDI values of TPUs were in the range of 1.65–1.82, which are highly consistent with the molecular weights. The low PDI values indicate that the prepared TPU samples have a narrow molecular weight distribution. However, some of the materials have a PDI lower than 1.70 (the theoretical value for linear step-growth polymers according to Flory's theory is 2), [38] which might suggest that the conversions of polymerizations are not sufficiently high for a one-shot bulk reaction. In the case of MP-2.5 and 3.0, PDI is closer to 2, so MDI is better for one-shot bulk polymerization reaction with a short polymerization time. This is true for almost of the TPUs, and it is nevertheless enough for polymer processing (injection and extrusion) and various other applications. These phenomena lead to differences in the TPU FT-IR spectra, DSC thermograms, and mechanical properties, as discussed below.

Chemical structure characterization

The chemical structures of the synthesized TPUs were obtained through Fourier transform infrared (FT-IR) spectroscopy. As shown in Fig. 1, all the obtained materials showed the presence of the characteristic groups typical for TPUs. There was no absorption band at 2270 cm^{-1} related to the NCO groups, thus indicating that the polyurethane reaction between hydroxyl and isocyanate groups occurred completely [12]. The N–H bond stretching vibration of urethane groups

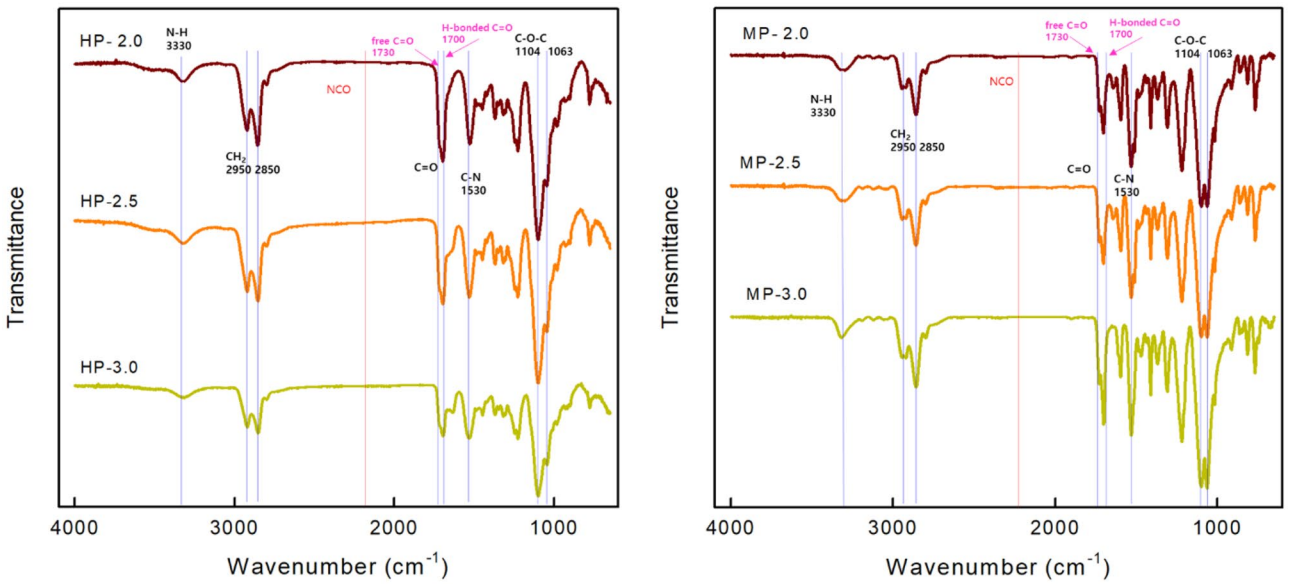

Fig. 1 FT-IR spectra with relation to characteristic groups in TPUs

appears at 3330 cm^{-1} due to the presence of hydrogen bonding. It is known that the N–H bond can be observed in two separate bands: hydrogen-bonded N–H at 3275–3300 cm^{-1} [39] and the free N–H bond at 3500 cm^{-1} [40]. The C-H asymmetric and symmetric stretching vibrations in the -CH_2 groups were observed as bimodal bands with the maxima at 2850 and 2950 cm^{-1}, respectively [41]. The double band observed in the range of 1680–1740 cm^{-1} corresponds to the carbonyl group (C=O) stretching vibrations [42, 43]. FT-IR spectrum analysis is a particularly useful tool for characterizing the variations in the functional groups of TPU, such as carbonyl (C=O) groups from urethane. The most common strong interaction in polymers and one that is essential to the properties and phase behavior of a range of important materials is hydrogen bonding. FT-IR is uniquely sensitive and considered to be diagnostic for, the formation of such bonds, and we have explored the use of this technique to quantitatively measure the fraction of hydrogen–bonded groups in polyurethanes. The intermolecular hydrogen–bonds significantly affect the degree of phase separation (DPS) of TPU. The FT-IR spectra for TPUs are displayed in Fig. 1 while the degrees of hydrogen–bonds calculated using Eq. (1) [44] are summarized in Table 3. The results show that the H-bonded C=O only exists in HS while free C=O is merely scattered in SS. Therefore, DPS could be calculated based on the amounts of free carbonyl bonded and H-bonded –C=O in the amorphous and ordered regions. The band observed at 1530 cm^{-1} is connected to the stretching vibration of the –CN bonds of the urethane groups [45]. The strong absorption band appearing at 1104 cm^{-1} is attributed to the free ether bond (C–O–C) of the used polyether polyol. The band maximum associated with the antisymmetric stretching vibrations of the non-associated ether group is found at the band of 1104 cm^{-1}, while the band of 1063 cm^{-1} is related to the hydrogen bond interaction between N–H and C–O–C groups [46].

$$\text{DPS (Degree of phase separation)} : R/(R+1) \quad (1)$$

$$R = \frac{\text{Ab(Absorption intensity of hydrogen bonded C = O)}}{\text{Af(Absorption intensity for free C = O)}}$$

$$\text{DPM (Degree of phase mixing)} : 1 - \text{DPS}$$

The [NCO]/[OH] molar ratio The N–H bond stretching vibration of urethane groups that appears at 3330 cm^{-1} is due to the presence of hydrogen bonding. It is commonly known that the N–H bond can be observed in two separate bands: hydrogen-bonded N–H at 3275–3300 cm^{-1} and the free N–H bond at 3500 cm^{-1}. The intensity of the N–H bond vibration increased as the [NCO]/[OH] molar ratio applied during polymerization decreased. This region also shows a little shoulder at 3500 cm^{-1} in all the curves, which corresponds to the non–H–bonded N–H group [47]. The formation of hydrogen bonds leads to the creation of HS, which is conducive to the process of micro–phase separation. Therefore, the fraction of hydrogen–bonded HSs is a relative measure of the degree of phase separation in TPUs. As presented in Table 3, there were only small differences in DPS among the materials containing different [NCO]/[OH] molar ratios. DPS slightly increased with increasing [NCO]/[OH] molar ratio, in correlation with the increasing hard segment content. According to the available literature, materials with higher HS contents are characterized by better microphase separation because of the increased long-range connectivity of HS, which can cause the formation of interconnected hard phase [48]. These results indicate that, in the case of HP and MP, the DPS increased with the increased [NCO]/[OH] molar ratio in the same way, and this result can be expected to affect the physical properties of the prepared film.

The kind of isocyanate In the case of the MP-3.0 (R = 1.67) sample, 62.5% of hard segments relate to hydrogen bonds. For the HP-3.0 sample (R = 1.25), slightly fewer hydrogen bonds were generated in the sample, with some limitations on the phase separation function depending on the isocyanate type. Further increasing the amount of isocyanate to create HS phase favors the elevation of the hydrogen bonds bonding the hard segments, as indicated by the corresponding increase in the R index. Prior research has shown that materials with a higher content of the hard segments possess more urethane groups [49]. Comparing the HP-3.0 and

Table 3 Deconvolution of the FT-IR absorbance bands in the range between 1750 and 1680 cm^{-1} occurring in the prepared TPUs

Sample	HS	Absorption intensity of C=O band		R	DPS	DPM
		Free C=O 1730 cm^{-1}	H-bonded C=O 1700 cm^{-1}			
HP-2.0	36.4	32.233	37.409	**1.16**	**0.537**	0.463
HP-2.5	41.0	27.480	32.486	**1.18**	**0.542**	0.458
HP-3.0	45.1	19.237	19.237	**1.25**	**0.555**	0.445
MP-2.0	32.6	28.100	45.160	**1.61**	**0.616**	0.384
MP-2.5	37.0	27.420	44.520	**1.62**	**0.619**	0.381
MP-3.0	40.8	23.620	39.410	**1.67**	**0.625**	0.375

MP-3.0 samples, the MP-3.0 sample shows higher DPS (0.625) despite having lower HS content. These groups can connect with the ether groups from polyols, thus increasing the interactions between HS and SS and prompting phase separation. In the MP-2.0 sample, it could be concluded that more than 60% of the HS was microphase separated, while only 40% of the HS seemed to be mixed within the polyether polyol matrix. However, the amount of H-boned C = O groups was affected not only by the HS content but also by the type of isocyanate. In conclusion, DPS slightly increased for TPUs prepared with the MDI as isocyanate. A correlation between band intensity and isocyanate type was observed with the higher peak at 1063 cm^{-1} with the MDI. Bistric et al. [50] prepared poly(ether-urethane)s based on MDI, poly(tetramethylene)glycol (Mw = 1000 g/mol) and BDO that had 34 and 51% of HS and showed from 0.61 to 0.69 of DPS, respectively. This dependence was confirmed by Niemczyk et al. [51]. Kasprzyk et al. [52] synthesized poly(ether-urethane)s, which showed 0.6 of DPS value. Fuensanta and Martín-Martínez [53] synthesized TPU with mixture of polyethers, that indicates lower degree of phase separation between the hard and soft domains in strongly dependent on the content of hard segments and used polyol.

Thermal analysis

Differential Scanning Calorimetry (DSC) was conducted to investigate the thermal behavior of the obtained TPUs and confirm their segmented structures. The thermal effects such as the glass transition of flexible segments, melting, and crystallization (including cold crystallization) were recorded and are presented here as endothermic and exothermic curves. The DSC thermograms generally showed three types of transitions for TPU: the glass transition temperatures of the SS/HS and the melting temperature of the HS/SS. Figure 2 shows DSC curves of the MP and HP series, and the results are summarized in Table 4. When considering the thermal analysis of TPU, it is necessary to examine the transition temperatures according to SS and HS phase separation. In a typical process, due to the thermodynamic incompatibility between the SS and the HS, phase separation occurs in the TPU materials, which results in separated peaks in T_g, T_m of SS and T_g, T_m of HS [54]. In a TPU with perfect phase separation, the SS forms the continuous phase while the HS phase is dispersed in this continuous phase in the form of lamellae, spherulites, etc., which act as physical cross-linkers [44]. Depending on the degree of phase separation, the transition temperatures may or may not appear clearly. The glass transition of the SS is dependent on the molecular weights of the polyols, types of raw materials used, and contents of the HS [55].

The [NCO]/[OH] molar ratio In terms of [NCO]/[OH] ratio, the T_g of HP-series decreases with the [NCO]/[OH] ratio, while the opposite occurs for MP-series. In the case of HP-series, this is interpreted to be a result of the increasing miscibility of the HS and SS and to indicate the presence of partial mixing of the HS within the SS microphase. The

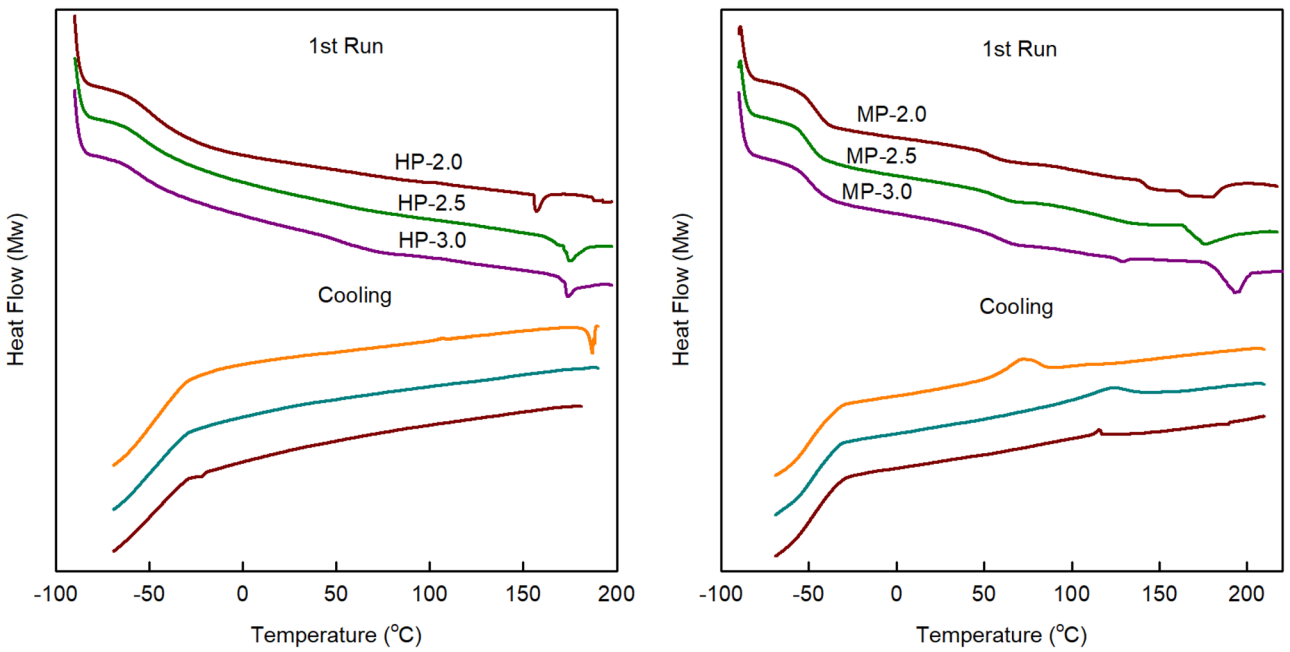

Fig. 2 Differential scanning calorimetry of first heating ramp measured at 20 °C/min from −100 °C to 200 °C for the sample series based on TPUs

Table 4 Summary of DSC results of bio-based TPUs

Sample	SS T_g(℃)	SS T_m(℃)	T_c(℃)	HS T_g (℃)	HS T_m(℃)	ΔH (J/g)
HP-2.0	–48.2	-		-	156.9	0.91
HP-2.5	–54.1	-	-	-	174.9	2.74
HP-3.0	–54.4	-	-	-	173.7	2.23
MP-2.0	–50.4	52.5	71.0	141.1	145.2	2.31
					165.7	
					179.6	
MP-2.5	–47.4	66.0	120.7	-	175.7	4.92
MP-3.0	–46.1	67.8	115.7	128.7	192.9	6.64

sample of the MP-series presented a higher T_g of SS, as higher contents of HS are well phase-separated, therefore increasing the DPS, as confirmed by FT-IR analysis. Moreover, since the T_g of SS is strongly dependent on the degree of miscibility between HS and SS [56, 57], the T_g is shifted toward higher temperatures with increasing HS content. This T_g shift may be explained by the increasing amount of HS "mixed" in the soft matrix. Further, the T_g of HS observed around 130–140 ℃ on MP-series could originate from a HS–rich phase separation, or longer HS, as the HS average length increases with higher HS content; [58, 59] it could also stem from a mix of both situations. This may be indicative of a kinetically favorable and stable phase separation.

The DSC cooling curves provide information about the crystallization behaviors of the TPUs. The decrease in [NCO]/[OH] substantially promoted the crystallization kinetics of the bio-based TPUs, while lower [NCO]/[OH] was shown to lead to broader peaks (higher DPM by FT-IR), as evidenced by the DSC's crystallization peaks. Sample MP-2.5 showed a 50 ℃ higher crystallization temperature (T_c) than sample MP-2.0. The T_m of SS was slightly increased as [NCO]/[OH] increased. The length of HS blocks forms the upper limit to the size of the HS crystals in the chain direction, which in turn determines the melting point and thus the thermal stability. As shown in Fig. 2, the temperature range in which most HS melts is seen to shift toward a higher temperature as the HS content increases. The T_m values at higher temperatures (155 ℃–192 ℃) related to the dissociation of a long-range ordering, which was related to mixing between HS and SS. These multiple peaks at higher temperatures were also associated with the melting of HS crystallites, phase separation into different domain sizes, and microcrystalline structures [51, 60]. In particular, samples of MP-2.0, MP-2.5, and MP-3.0 showed increased high-temperature T_m peaks along with shifts to higher temperatures, which were attributed to better HS ordering and the formation of stronger and more stable HS domains. Moreover, these samples also showed defined bimodal T_c behaviors, thus indicating the formation of more than one crystallite type.

The kind of isocyanate The phase separation between HS and SS depends on their respective lengths and affinity for each other, which is closely related to their abilities to establish hydrogen bond interactions. As a result, it is affected by the chemical composition and HS content in the synthesized TPUs. In this way, the slight increase in T_g observed for the MP-series means that there is only a relatively large amount of HS mixed within the soft domain, thus resulting in a higher degree of microphase separation for this TPU series, owing to the increase of molecular weight and crystallinity. These results are consistent with the FT-IR spectra in the C = O region, which show the involvement of hydrogen-bonded and free carbonyl groups. The crystallinity and T_m of the hard phase are drastically affected by the HS length distribution. Various researchers [15, 55, 61, 62] have shown that the properties of TPUs can be improved by using uniform HS, as these lead to more complete phase separation. Isocyanate type was found to affect the T_m of TPUs at a higher temperature using MDI. The melting of HS was registered as multiple melting endotherms (MME) in the MP-2.0 sample. MME can be attributed to distinct crystal populations with different melting temperatures linked to thermal history. In the case of high SS content, it was shown that the MME were due to SS rich-micro-domains that appeared in a hard ordered phase in materials based on MDI. There was also disordering in the HS, as well as partial miscibility of the hard phase in SS, as confirmed by the decrease in crystallization [63, 64]. The differences in the T_m behaviors of the TPU materials suggest that they have different physical origins. The lower temperatures can be attributed to the melting of suitable or less-ordered structures of SS, but the higher temperatures are associated with greater-order structures. The materials obtained from the aromatic isocyanates show a higher glass transition temperature than the materials obtained from the aliphatic isocyanates. The lower glass transition temperatures observed for TPUs obtained using the aliphatic isocyanates are a result of the improved separations of the phases [65–68]. The presence of an aromatic isocyanate in the HS produces a stiffer polymer chain with a higher melting point.

Dynamic mechanical thermal analysis (DMA) The results of dynamic mechanical thermal analysis are presented in Fig. 3 and Table 5 as a functional relationship of the storage modulus (G′), loss modulus (G″) versus temperature. The storage modulus defines the energy stored elastically by the materials at deformation, and it provides information about the polymer stiffness [69]. The T_g was expressed as the temperature at which the loss modulus G″ reaches its maximum. The T_g of TPU can be detected by both DSC and DMA, and the T_g values found by both analysis methods are similar to each other. However, no melting transition can be detected in the DSC thermogram, while at least the flow behavior of TPU can be observed in the DMA. The results show that there was a low T_g of the SS; a high T_{flow} due to the melting of the HS; a high modulus at very low temperatures (−100 °C); a lower modulus above the T_g of the SS phase, which was only slightly temperature-dependent; and a low loss modulus. In the rubbery plateau region, the modulus above the T_g of the SS depends on the reinforcing effect of the HS on the soft matrix [44]. The storage modulus of G'_{25} increased significantly as the HS content increased. With phase-separated HS, the modulus increased significantly with higher HS content, thus causing the materials to become stiffer. The flex temperature (T_{flex}) is defined as the temperature at the start of the rubber plateau region, which is the intercept of the tangents. The flow temperature (T_{flow}) was defined as the temperature where the storage modulus G′ reached 1 MPa; the storage modulus of the rubbery plateau is determined at room temperature. The modulus at the rubbery plateau in the $T_{flex} - T_{flow}$ region is a function of the HS crosslink density and reinforcement by the separated HS. TPUs from segmented copolymers can typically be made with a range of rubbery modulus values by changing the hard segment content [58].

Table 5 Summary of DMA results of bio-based TPUs

Sample	T_g (℃)	G'_{25}(MPa)	T_{flex} (℃)	T_{flow} (℃)
HP-2.0	-53	3.99	28.0	85
HP-2.5	-54	8.81	57.0	122
HP-3.0	-54	34.65	72.0	149
MP-2.0	-47	10.53	21.4	136
MP-2.5	-43	13.54	23.6	133
MP-3.0	-43	24.50	28.7	173

The [NCO]/[OH] molar ratio As the [NCO]/[OH] molar ratio increased, the T_{flow} of the corresponding TPU increased from 85 to 149 °C. These T_{flow} results are due to the melting of the phase-separated HS, and the observed increase in T_{flow} may be the result of increased hydrogen bonding in the HS domain [70]. The T_{flow} decreases with decreasing HS content. The materials with the highest content of HS were characterized by the broadened peak of the storage modulus due to the limitations of the soft segment flexibility [71]. This result is consistent with those that have been obtained using other systems.

The kind of isocyanate The T_{flow} of the MP-series is considerably higher than that of the HP-series. This phenomenon has been attributed to the solvent effect theory of Flory [72]. In MP-series, the rubbery plateau is extended, and it displays a higher rubbery modulus and sharper peak than HP-series. The constant value of this storage modulus indicates that

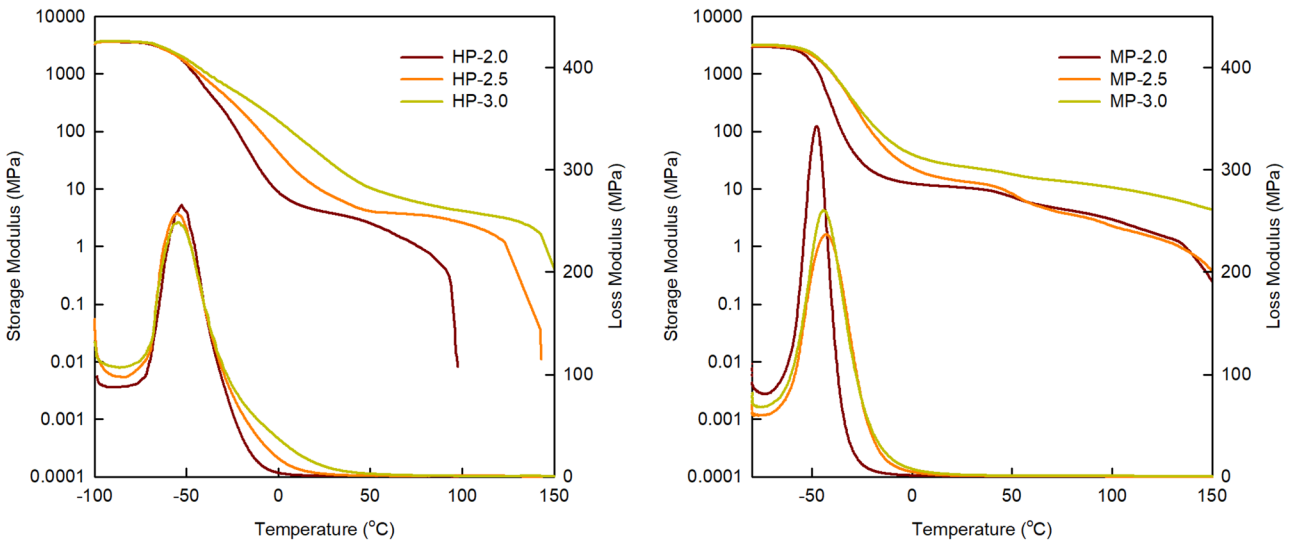

Fig. 3 Storage modulus (G′), loss modulus (G″) versus temperature for the obtained bio-based TPUs

no phase transitions occur within this temperature range, and that phase separation is more effective. These results are attributed to the existence of a higher degree of phase separation in the samples of the MP-series due to the higher DPS, as indicated by the FT-IR results.

The structural proposal in Fig. 4 was supported by the segmented structure of TPU, which can serve as a guideline to elucidate the morphology of these polymers. The size and shape of the hard domains in the TPU were evaluated using atomic force microscopy (AFM) [73–76]. The samples exhibited two types of phase contrast: a dark, featureless matrix corresponding to the SS and bright elements [76]. The shape of the hilly was significantly different when the HP-series and MP-series were compared. 3D AFM images show the surface physical structure and quantify the surface roughness (R_a). Accordingly, R_a was observed 180, 1177 nm of HP-series and MP-series respectively. The HP-series showed a sharp hilly, whereas a more rounded hilly was observed in the MP-series. The MP-series show the largest hilly surface with large globules and the high roughness value. These characteristics are affected by the isocyanate type, and micro-phase separation of the HS and SS.

This is an advantage compared to other thermoplastic elastomers, which often show a decrease in the rubbery plateau region with increasing temperature because of incomplete phase separation or partial melting of the HS. The MP-series showed high values for T_g, G'_{25}, T_{flex}, and T_{flow} as compared to the HP-series. The regions of rubbery plateau between T_{flex} and T_{flow} were further extended as well. Typically, because of the thermodynamic incompatibility between the SS and the HS, phase separation occurs in the TPU materials, which results in elastomeric properties.

Thermogravimetric analysis (TGA) curves for TPUs prepared under different conditions are shown in Fig. 5 while the corresponding data are summarized in Table 6.

The [NCO]/[OH] molar ratio Four stages of thermal degradation could be observed for all the TPUs. The temperature of 5wt % weight loss (T5) is typically considered as the onset decomposition temperature. The results showed differences at the beginning of thermal degradation (T5) depending on the [NCO]/[OH] molar ratio. It could also be seen that with increasing [NCO]/[OH] molar ratio, molecular weight and T5 increased. Despite the presence of a single-step drop, there are two peaks in the derivative curve (%/°C) due to a change in the curve slope as it descends; TPUs present two decomposition stages: a first step at 330–370 °C which is related to HS decomposition and a second step around 425 °C which is related to SS decomposition [42]. All TPUs prepared in this work showed this characteristic, and the rate of weight loss was dependent on [NCO]/[OH]. With the increase in [NCO]/[OH], the maximum weight loss rate for the first and second decomposition step decreases. All TPUs with a higher HS content also showed a higher weight loss rate for the first decomposition step and a lower weight loss rate for the second decomposition step. In conclusion, an increase in [NCO]/[OH] led to a corresponding increase in thermal stability.

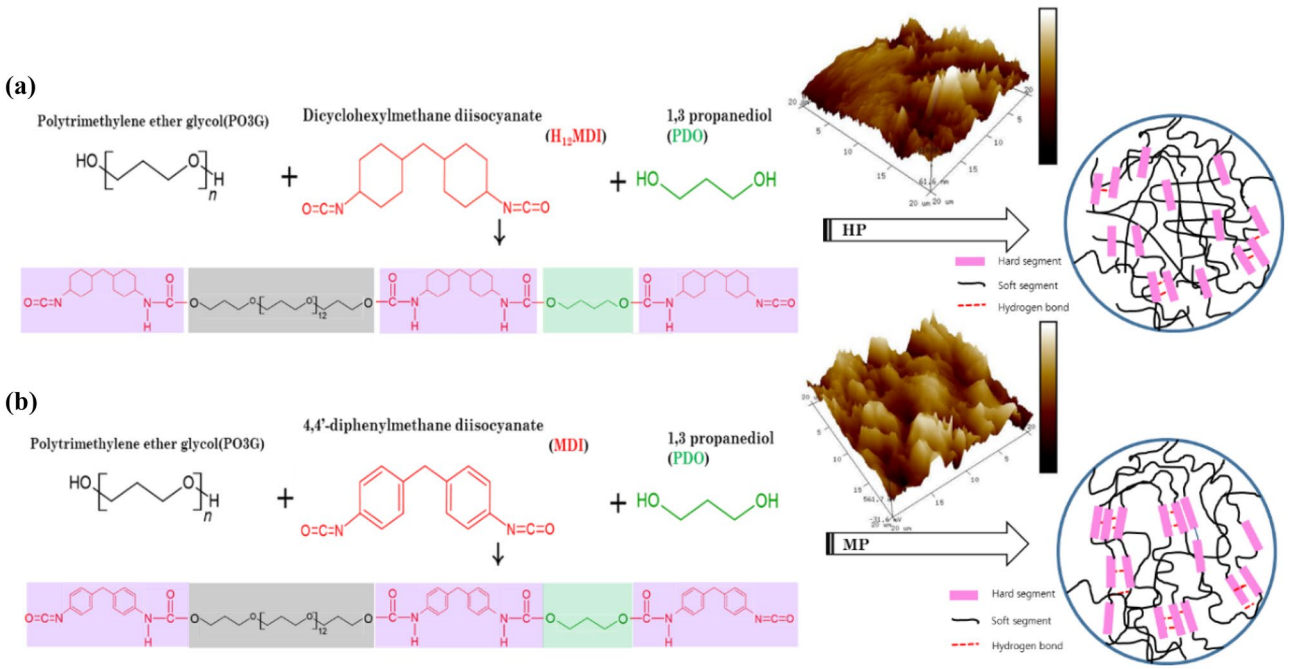

Fig. 4 A schematic representation of the bio-based TPU with two types of isocyanate

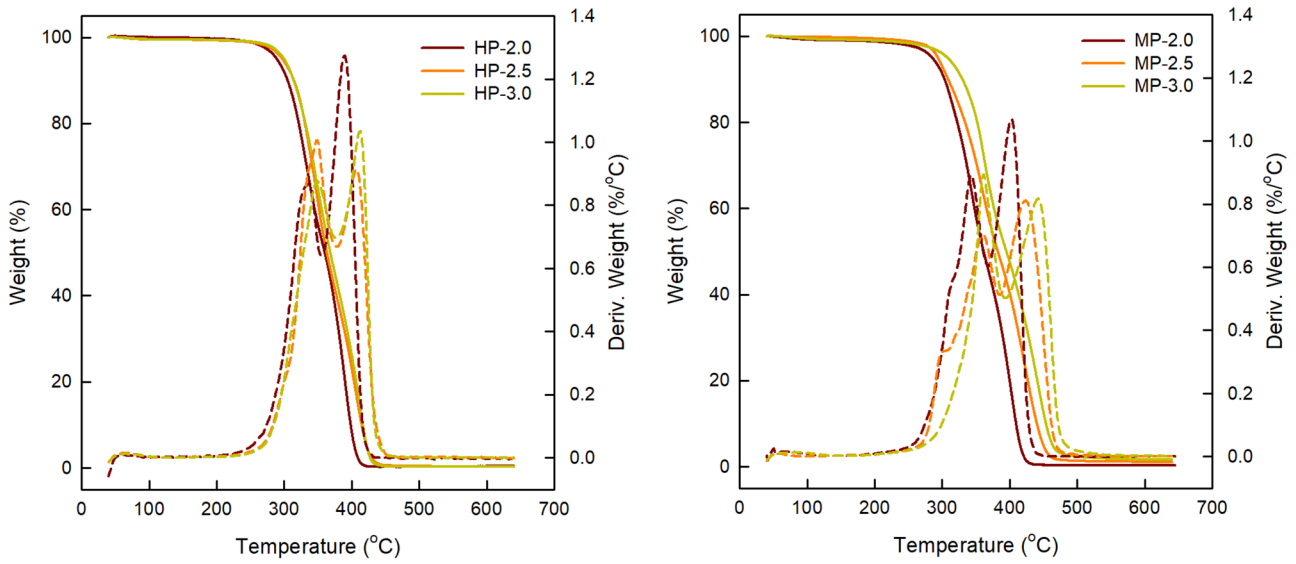

Fig. 5 TGA curves and their derivative curves of bio-based TPUs

The kind of isocyanate As a general trend, MP-series showed T5% that were 10 °C higher than those of HP-series. In particular, the MP-3.0 sample is characterized by the best thermal stability in the initial stage of decomposition. Thus, in MP-3.0, higher temperatures are needed to obtain 5 and 10% weight loss than are needed in other materials. From the point of view of thermal properties, it is therefore advantageous to use MDI as isocyanate. This relationship was reversed in the first step of degradation (T_{HS}) at a higher temperature, which suggests a more cross-linked structure of the polymer. Further, the materials obtained from aromatic isocyanate show higher thermal stabilities than materials obtained from aliphatic isocyanate. It was therefore found that the type of isocyanate has a greater effect on thermal stability.

Mechanical properties

Figure 6 and Table 7 lists the mechanical properties for all the samples at room temperature (initial modulus, tensile strength, and elongation at break) and hardness (Shore A).

Table 6 Thermal decomposition characteristics of the obtained bio-based TPUs

Sample	T5% (℃)	T10% (℃)	T50% (℃)	T_{HS} (℃)	T_{SS} (℃)
HP-2.0	289.3	305.3	360.2	335	388
HP-2.5	297.5	314.7	363.5	350	404
HP-3.0	299.8	314.2	368.6	352	410
MP-2.0	285.3	303.7	361.4	340	404
MP-2.5	293.9	308.9	382.5	361	425
MP-3.0	308.1	330.1	395.2	361	442

The mechanical performances of TPUs are closely related to their compositions; in general, HS could act as physical crosslinks and reinforcing units, while SS is responsible for the material flexibility due to the long linear polyol chain.

The [NCO]/[OH] molar ratio From the data in Table 6, it can be concluded that the bio-based thermoplastic poly(etherurethane)s prepared with the highest [NCO]/[OH] molar ratio have the highest content of HS. The initial modulus values of HP-series and MP-series respectively ranged from 446.42–2146.28 MPa and from 145.58–1039.92 MPa. Therefore, the initial modulus values increased with the amount of HS contents in the polymer, which was associated with higher stiffness and content of hard segments [42]. The same relationships were shown for all prepared samples with respect to tensile strength and elongation at break. The increase in HS content from 37.1 to 46 wt% resulted in a corresponding increase in tensile strength from 3.29 to 23.45 MPa. The increase in [NCO]/[OH] molar ratio also led to higher tensile strength. The HS content also determines the tensile strength, while the SS content relates to the elongation at break values. The elongation at break is also related to the decrease in the chain mobility, and the permanent set after the break suggests the possibility of macromolecular chains returning to the states in which they were before the test [77]. The HP-2.0 displayed the highest elongation at break (1718%) as well as tensile strength values above 20 MPa. Meanwhile, the HP-3.0 showed higher hardness (Shore A) than HP-2.0. Thus, the value of hardness increased as the content of hard segments increased, which is suggested by the FTIR data to be due to the higher stiffness of these materials. Hardness also increased with

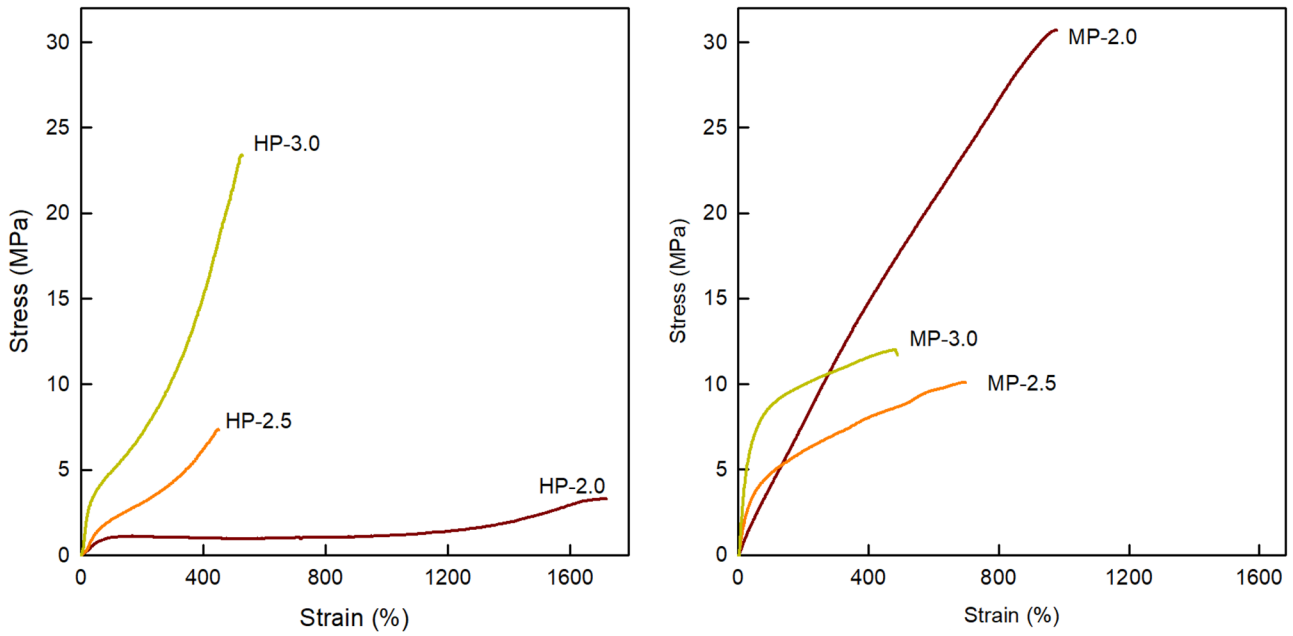

Fig. 6 Tensile stress–strain curves of the bio-based TPUs

increasing [NCO]/[OH] molar ratio. The samples of HP2.0, HP2.5, and HP3.0 showed elongations at break of 1718, 450, and 528%, respectively. These differences in the elongation at break are related to decreases in the chain mobility, which was confirmed for the HP-series by the shifting of the T_g temperature to higher values. Hardness is closely connected with the crosslink density in HS. This resulted in the reduced elasticity of the samples, which led to more rigid materials. The MP-series had the highest hardness, with values ranging from 71 to 79 Shore A. As the crosslink density increases, the stiffness of the materials increases as well. Available literature presents a lot of studies about thermoplastic poly(ether-urethane)s. The most of presented TPUs based on poly ether polyols showed tensile strength in the range from 4 to 40 MPa, elongation at break up to 900%, hardness up to 30 °ShD, and Young's modulus in the range from 18 to 60 MPa. Materials obtained in this work possess mechanical properties comparable with other presented works [7, 13, 18, 49, 50]. Kasprzyk and Datta [36] investigated bio-ether based TPU that presented tensile strength 5–19 MPa, elongation at break up to 590%, hardness up to 36°ShD. According to Zhang et al. [24] among the mechanical properties of TPU film using castor oil, tensile strength was 11 MPa, elongation at break up to 233%, the thermal properties were $T_{10\%}$ = 275 °C, and T_{HS} / T_{SS} = 290 °C/350 °C.

The kind of isocyanate The tensile strength and elongation at break of bio-based TPUs obtained using MDI as isocyanate respectively ranged from 30.69 to 11.07 MPa and from 977 to 489%. The hardness of a material is its ability to resist deformation, indentation, or scratching. Shore A tests are the most common method used to measure the hardness of TPUs, and their results are related to the initial modulus; as the initial modulus increases, the Shore A values also tend to increase. Because of their block copolymer nature, TPUs with hardness values between Shore 60A and 85A can be obtained by varying the ratio of HS to SS. The hardness,

Table 7 Mechanical properties and hardness of TPUs

Sample	Initial Modulus (MPa)	Tensile strength (MPa)	Elongation (%)	Energy(J)	Shore A
HP-2.0	145.58 ± 0.73	3.29 ± 0.02	1718.6 ± 8.59	0.26 ± 0.001	59
HP-2.5	266.82 ± 1.33	7.34 ± 0.04	450.7 ± 2.25	0.13 ± 0.001	78
HP-3.0	1039.92 ± 5.20	23.45 ± 0.12	528.7 ± 2.64	0.91 ± 0.005	84
MP-2.0	446.42 ± 2.23	30.69 ± 0.15	977.8 ± 4.89	2.41 ± 0.012	71
MP-2.5	1062.12 ± 5.31	10.07 ± 0.05	698.4 ± 3.49	0.37 ± 0.002	73
MP-3.0	2146.28 ± 10.73	11.07 ± 0.06	489.9 ± 2.45	0.53 ± 0.003	79

modulus, load-bearing capacity (compressive stress), and strength of TPUs typically increase with increasing HS content. TPU obtained using H_{12}MDI is more flexible and has a higher elastic modulus and tensile strength than TPU obtained using MDI. The HS of TPU prepared using MDI were more hydrogen bonded and phase separated than those of HS contained H_{12}MDI, which showed stiffer and stronger polymers.

Conclusions

Recently, there has been increased interest in developing bio-based polyols and TPUs owing to the environmental issues, which will lead to a growing demand for materials with soft and strong properties. In order to meet these demands of the times, this study aimed to synthesize a bio-based TPU. We used bio-based polytrimethylene ether glycol (PO3G) as a polyol, 1-isocyanato-4-[(4-isocyanatophenyl)methyl]benzene (MDI) and 1,1'-methylenebis(4–isocyanatocyclohexane) (H_{12}MDI) as the isocyanate, and bio-based propane-1,3-diol (PDO) as the chain extender. Bio-based TPUs with [OH]/[NCO]/[OH] molar ratios ranging from 1:2:1 to 1:3:1 was successfully synthesized using a solvent-free one-shot process. **Considering the [NCO]/[OH] molar ratio,** the M_w of TPUs increased in the ranges from 44,160–60,141 g/mol. The degree of phase separation (DPS) also increased, and it is expected that this result will affect the thermal and physical properties of the prepared film. **Considering the isocyanate type,** the MDI-based TPU samples showed higher average molecular weight and degree of phase separation (DPS) than H_{12}MDI-based TPU samples, despite having a lower content of HS. Due to these results, the MP samples have better ordered, stronger, and more stable HS domains. SS T_g, SS T_m, T_c, HS T_g, and HS T_m of MP-3.0 were shown by DSC analysis at –46.09 °C, 67.84 °C, 115.7 °C, 129.69 °C, and 192.92 °C, respectively. T_{flex} and T_{flow} of MP-3.0 were found by DMA analysis to be 28.7 and 173 °C, respectively. According to TGA, the materials obtained from aromatic isocyanate showed higher thermal stability than materials from aliphatic isocyanate. The mechanical properties of MP-series can be seen to be higher than those of HP-series. From the previous results, it was found that when an aromatic isocyanate (MDI) was used when synthesizing TPU with a bio-based ether polyol, a sample having excellent thermal and physical properties that was also soft could be obtained. These findings of this study are expected to contribute to the preparation of fused deposition modeling (FDM) 3D printing or 4D printing for shape memory polymer from bio-based TPU filaments for use in soft actuators with a shore hardness range of 59~84A. In the future, we would like to investigate whether these TPU sample values are suitable for FDM 3D printing filaments for soft actuators as well as investigate the properties of the filaments using an extruder and whether these TPU samples can be used as a shape memory polymer for 4D printing filaments. 4D printing of actuator provides a good chance to access stimulus-responsive soft robots for potential applications. Owing to the advantages of customized and personalized fabrication of bio-related materials, 4D bioprinting shows great potential in biomedical applications. For example, tailor-made suture, ischemic stroke devices, vascular repair device, and theragrippers can be achieved by 4D printing.

Supplementary Information The online version contains supplementary material available at https://doi.org/10.1007/s10965-022-03375-x.

Acknowledgements This work was supported by the National Research Foundation of Korea (NRF) grant funded by the Ministry of Science and ICT of Korea government (MSIT) (No. NRF-2021R1A4A1022059)

Data availability The data presented in this study are available on request from the corresponding author.

References

1. Delibes E, Pascault JP, Boutevin B, Ganachaud F (2013) On the versatility of urethane/urea bonds: reversibility, blocked isocyanate, and non-isocyanate polyurethane. Chem Rev 113:80–118
2. Panel M, Charlonab B, Heinrichc Y, Matterab E, Couzignéc B, Donniocd L, Avérousa (2014) Synthesis, structure, and properties of fully biobased thermoplastic polyurethanes, obtained from a diisocyanate based on modified dimer fatty acids, and different renewable diols. Eur Polym J. 61:197–205
3. Zhu Y, Romain C, Williams CK (2016) Sustainable polymers from renewable resources. Nature 540:354–362
4. Ji S, Cao W, Yu Y, Xu H (2015) Visible-Light-Induced Self-Healing Diselenide-Containing Polyurethane Elastomer. Adv Mater 27:7740–7745
5. Harrell LJ (1969) Segmented polyurethanes. Properties as function of segment size and distribution. Macromolecules 2:607–612
6. Ng H, Allegrezza A, Seymour R, Cooper L (1973) Effect of segment size and polydispersity on the properties of polyurethane block copolymers. Polymer 14:255–261
7. Holden G, Kricheldorf R, Quirk P (2004) Thermoplastic elastomer, 3rd edn. Hanser, Munich
8. Alagi P, Choi Y, Hong J (2016) Preparation of vegetable oil-based polyols with controlled hydroxyl functionalities for thermoplastic polyurethane. Eur. Polym. J. 78:46–60
9. Fakirov S (2005) Handbook of condensation thermoplastic elastomer. Wiley-VHC Verlag, Weinheim

10. Xu W, Zhang R, Liu W, Zhu J, Dong X, Guo H, Xand A (2016) Multiscale investigation on the mechanism of shape recovery for IPDI to PPDI hard segment substitution in polyurethane. Macromolecules 49:5931–5944
11. Lunardon G, Sumadia Y, Vogl O (1980) Effects of molecular-weight and molecular weight distribution of polyester based soft segments on the physical-properties of linear polyurethane elastomers. Angew Makromol Chem 87:1–33
12. Kasprzyk P, Datta J (2019) Novel bio-based thermoplastic poly (ether-urethane) s. Correlations between the structure, processing and properties. Polymer 160:1–10
13. Ferrer M, Babb D, Ryan A (2008) Characterisation of polyurethane networks based on vegetable derived polyol. Polymer 4932:79–87
14. Husken D, Feijen J, Gaymans R (2007) Hydrophilic segmented block copolymers based on poly(ethylene oxide) and monodisperse amide segments. J Polym Sci Part A Polym Chem 45:4522–4535
15. Kull K, Bass R, Craft G, Julien T, Marangon E, Marrouat C, Harmon J (2015) Synthesis and characterization of an ultra-soft poly (carbonate urethane). Eur Polym J 71:510–522
16. Brydson J (1995) Plastic materials. Butterworth Scientific, London
17. Oertel G (1985) Polyuretane handbook. Hanser Publishers, Munich
18. Sawpan M (2018) Polyurethanes from vegetable oils and applications: a review. J Polym Res 25:1–15
19. Shen Y, He J, Xie Z, Zhou X, Fang C, Zhang C (2019) Synthesis and characterization of vegetable oil based polyurethanes with tunable thermomechanical performance. Ind Crops Prod 140:711–717
20. Petrovic Z, Yang L, Zlatanic A, Zhang W, Javni I (2007) Network structure and properties of polyurethanes from soybean oil. J Appl Sci 105:2717–2727
21. Zafar F, Ghosal A, Sharmin E, Chaturvedi R, Nishat N (2019) A review on cleaner production of polymeric and nanocomposite coatings based on waterborne polyurethane dispersions from seed oils. Prog Org Coat 131:259–275
22. Miao S, Sun L, Wang P, Liu R, Su Z, Zhang S (2012) Soybean oil-based polyurethane networks as candidate biomaterials: synthesis and biocompatibility. Eur J Lipid Sci Technol 114:1165–1174
23. Miao S, Wang P, Su Z, Zhang S (2014) Vegetable-oil-based polymers as future polymeric biomaterials. Acta Biomater 10:1692–1704
24. Shin EJ, Jung YS, Choi HY, Lee S (2022) Synthesis and fabrication of biobased thermoplastic polyurethane filament for FDM 3D printing. J Appl Polym Sci 139(40):e52959
25. Wehner M, Truby RL, Fitzgerald DJ, Mosadegh B, Whitesides GM, Lewis JA, Wood RJ (2016) An integrated design and fabrication strategy for entirely soft, autonomous robots. Nature 536(7617):451–455
26. Petrović ZS, Milić J, Zhang F, Ilavsky J (2017) Fast-responding bio-based shape memory thermoplastic polyurethanes. Polymer 121:26–37
27. Yusrizal AA, Abdullah TK, Ali ES, Ahmad S, Zubir SA (2022) Enhanced thermal and tensile behaviour of MWCNT reinforced palm oil polyol based shape memory polyurethane. Arab J Chem 15(7):103860
28. Madbouly SA (2022) Bio-based castor oil and lignin sulphonate: aqueous dispersions and shape-memory films. Biomater Polymers Horizon 1(1):1–14
29. Fernandes CD, Oechsler BF, Sayer C, de Oliveira D, de Araújo PHH (2022) Recent advances and challenges on enzymatic synthesis of biobased polyesters via polycondensation. Eur Polymer J 169:111132. ISSN 0014-3057. https://doi.org/10.1016/j.eurpolymj.2022.111132
30. Liu LY, Karaaslan MA, Hua Q, Cho M, Chen S, Renneckar S (2021) Thermo-Responsive Shape-Memory Polyurethane Foams from Renewable Lignin Resources with Tunable Structures-Properties and Enhanced Temperature Resistance. Ind Eng Chem Res 60(32):11882–11892
31. Li S, Jose J, Bouzidi L, Leao AL, Narine SS (2014) Maximizing the utility of bio-based diisocyanate and chain extenders in crystalline segmented thermoplastic polyester urethanes: Effect of polymerization protocol. Polymer 55:6764–6775
32. Gogoi R, Alam M, Khandal R (2014) Effect of increasing NCO/OH molar ratio on the physicomechanical and thermal properties of isocyanate terminated polyurethane prepolymer. Int J Basic Appl Sci 3:118–123
33. Fu B, MacKnight J, Schneider S (1986) Structure-properties of segmented polyurethanes containing monodisperse 2,4 toluene diisocyanate butane diol hard segments. Rubber Chem Techn 59:896–911
34. Camberlin Y, Pascault P, Letoffe M, Letoffé M, Claudy P (1982) Model hard segments from diphenyl methane diisocyanate and different chain extenders, and corresponding linear block polyurethanes. J Polym Sci Part A Polym Chem 20:1445–1456
35. Christenson P, Harthcock A, Meadows D, Spell L, Howard L, Creswick W, Guerra E, Turner B (1986) Model MDI/butanediol polyurethanes: molecular structure, morphology, physical and mechanical properties. J Polym Sci Part B Polym Phys 24:1401–1439
36. Kasprzyk P, Datta J (2018) Effect of Molar Ratio [NCO]/[OH] Groups during Prepolymer Chains Extending Step on the Morphology and Selected Mechanical Properties of Final Bio-Based Thermoplastic Poly (Ether-Urethane) Materials. Polym Eng Sci 58:E119–E206
37. Paulina K, Hynek B, Ricardo K, Donato, Janusz D (2020) The role of hydrogen bonding on tuning hard-soft segments in biobased thermoplastic poly(ether-urethane)s. J. Clean Prod 274:122678
38. Odian G (2004) Principles of polymerization. John Wiley & Sons, Hoboken
39. Kirpluks M, Cabulis U, Ivdre A, Kuranska M, Zieleniewska M, Auguscik M (2016) Mechanical and thermal properties of high-density rigid polyurethane foams from renewable resources. J Renew Mater 4(1):86–100
40. Coleman M, Lee K, Skrovanek D, Painter P (1986) Hydrogen bonding in polymers. 4. Infrared temperature studies of a simple polyurethane. Macromolecules 19(8):2149–2157
41. Lluch C, Esteve-Zarzoso B, Bordons A, Lligadas G, Ronda M, Galia CV (2014) Antimicrobial polyurethane thermosets based on undecylenic acid: Synthesis and evaluation. Macromol Biosci 14(8):1170–1180
42. Hongwei L, Nubla M, Zhen M, Mingqiang Z, Junqi W, Jilu Z, Zhongshun Y, Qin W, Charles (Chunbao) X (2017) Preparation and characterization of bio-polyol and bio-based flexible polyurethane foams from fast pyrolysis of wheat straw. Ind. Crops Prod 103:64–72
43. Tao Y, Hasan A, Deeb G, Hu C, Han H (2016) Rheological and mechanical behavior of silk fibroin reinforced waterborne polyurethane. Polymers 8(3):94
44. Van der Schuur M, Gaymans J (2006) Segmented block copolymers based on poly(propylene oxide) and mono disperse polyamide-6, T segments. J Polym Sci Part A Polym Chem 44:4769–4781
45. Gorna K, Polowinski S, Gogolewski S (2002) Synthesis and characterization of biodegradable poly(e-caprolactone urethane)s. I. Effect of the polyol molecular weight, catalyst, and chain extender on the molecular and physical characteristics. J Polym Sci Part A Polym Chem 40:156–170
46. Kalita H, Karak N (2014) Biobased hyperbranched shape memory polyurethanes: Effect of different vegetable oils. J Appl Polym Sci 131:1–8

47. Gurunathan T, Mohanty S, Nayak SK (2015) Isocyanate terminated castor oil-based polyurethane prepolymer : Synthesis and characterization. Prog Org Coatings 80:39–48
48. Klinedinst DB, Yilgör I, Yilgör E, Zhang M, Wilkes GL (2012) The effect of varying soft and hard segment length on the structure–property relationships of segmented polyurethanes based on a linear symmetric diisocyanate, 1,4-butanediol and PTMO soft segments. Polymer 53:5358–5366
49. Close G, Rabani H, Luftmann A, Kraft (2005) Synthesis and properties of segmented copolymers containing short aramid hard segments and aliphatic polyester or polycarbonate soft segments. Polymer 46:27–35
50. Bistričić L, Baranović G, Leskovac M, Bajsić EG (2010) Hydrogen bonding and mechanical properties of thin films of polyether-based polyurethane–silica nanocomposites. Eur Polym J 46:1975–1987
51. Niemczyk A, Piegat A, Sonseca Olalla Á, El Fray M (2017) New approach to evaluate microphase separation in segmented polyurethanes containing carbonate macrodiol. Eur Polym J 93:182–191
52. Kasprzyk P, Sadowska E, Datta J (2019) Investigation of thermoplastic polyurethanes synthesized via two different prepolymers. J Polym Environ 27(11):2588–2599
53. Fuensanta M, Martín-Martínez JM (2018) Thermoplastic polyurethane coatings made with mixtures of polyethers of different molecular weights with pressure sensitive adhesion property. Prog Org Coat 118:148–156
54. Spontak J, Patel P (2000) Thermoplastic elastomers: fundamentals and applications. Curr Opin Colloid Interface Sci 5:334–341
55. Saralegi A, Rueda L, Fernández-D'Arlas B, Mondragon A, Eceiza C (2013) Thermoplastic polyurethanes from renewable resources: Effect of soft segment chemical structure and molecular weight on morphology and final properties. Polym Int 62:106–115
56. Eceiza A, Martin MD, de la Caba K, Kortaberria GN, Gabilondo CI, Mondragon A (2008) Thermoplastic polyurethane elastomers based on polycarbonate diols with different soft segment molecular weight and chemical structure: mechanical and thermal properties. Polym Eng Sci 48:297–306
57. Niemczyk A, Piegat A, Sonseca Olalla Á, El F (2017) New approach to evaluate microphase separation in segmented polyurethanes containing carbonate macrodiol. Eur Polym J 93:182–191
58. Peebles H (1974) Sequence Length Distribution in Segmented Block Copolymers. Macromolecules 7:872–882
59. Peebles H (1976) Hard Block Length Distribution in Segmented Block Copolymers. Macromolecules 9:58–61
60. Hossieny N, Shaayegan V, Ameli A, Saniei M, Park CB (2017) Characterization of hard-segment crystalline phase of thermoplastic polyurethane in the presence of butane and glycerol monosterate and its impact on mechanical property and microcellular morphology. Polymer 112:208–218
61. Silva V, Mosiewicki A, Yoshida I, Silva M, Stefani PM, Marcovich NE (2013) Polyurethane foams based on modified tung oil and reinforced with rice husk ash I: synthesis and physical chemical characterization. Polym Test 32:438–441
62. Li C, Liu J, Li J, Shen F, Huang Q, Xu H (2012) Studies of 4,4′-diphenylmethane diisocyanate (MDI)/1,4-butanediol (BDO) based TPUs by in situ and moving-window two-dimensional correlation infrared spectroscopy: Understanding of multiple DSC endotherms from intermolecular interactions and motions level. Polymer 53:5423–5430
63. Jeffrey T, Koberstein AF (1992) Galambos Multiple melting in segmented polyurethane block copolymers. Macromolecules 25(21):5618–5624
64. Fernández-d'Arlas B, Jens B, Peter R, Pöselt E, Raphael BT, Müller A (2016) Tailoring the Morphology and Melting Points of Segmented Thermoplastic Polyurethanes by Self-Nucleation. Macromolecules 49(20):7952–7964
65. Saiani A, Daunch WA, Verbeke H, Leenslag JW, Higgins JS (2001) Origin of Multiple Melting Endotherms in a High Hard Block Content Polyurethane. 1. Thermodynam Investig Macromolec 34(26):9059–9068
66. Saiani A, Rochas C, Eeckhaut G, Daunch WA, Leenslag JW, Higgins JS (2004) Origin of Multiple Melting Endotherms in a High Hard Block Content Polyurethane. 2. Struct Investig Macromolec 37(4):1411–1421
67. Saiani A, Novak A, Rodier L, Eeckhaut G, Leenslag J-W, Higgins JS (2007) Origin of Multiple Melting Endotherms in a High Hard Block Content Polyurethane: Effect of Annealing Temperature. Macromolecules 40:7252–7262
68. Bueno-Ferrera C, Elodie H, María G, Sergio B, Luc A, Alfonso J (2012) Relationship between morphology, properties and degradation parameters of novative biobased thermoplastic polyurethanes obtained from dimer fatty acids. Polym Degrad Stab 97:1964–1969
69. Lei W, Fang C, Zhou X, Cheng Y, Yang R, Liu D (2017) Morphology and thermal properties of polyurethane elastomer based on representative structural chain extenders. Thermochim Acta 653:116–125
70. Biemond E, Feijen J, Gaymans J (2009) Segmented block copolymers with monodisperse hard segments: the influence of H-bonding on various properties. Macromol Mater Eng 294:492–501
71. Ugarte L, Fernández-d'Arlas B, Valea A, González ML, Corcuera MA, Eceiza A (2014) Morphology–properties relationship in high-renewable content polyurethanes. Polym Eng Sci 54:2282–2291
72. Flory J (1942) Thermodynamics of High Polymer Solutions. J Chem Phys 10:51
73. Kultys A, Rogulska M, Pikus S, Skrzypiec (2009) The synthesis and characterization of new thermoplastic poly(carbonate-urethane) elastomers derived from HDI and aliphatic-aromatic chain extenders. Eur Polym J 45(9):2629–43
74. Kojio K, Kugumiya S, Uchibaq Y, Nishino Y, Furukawa M (2009) The micro-separated structure of polyurethane bulk and thin films. Polym J 41(2):118–124
75. Long J, Jia W, Chinemelum N, Alberto S, Hazel EA (2015) Phase separation and crystallization in high hard block content polyurethane thin films. Macromolecules 48(15):5358–5366
76. Špírková M, Strachota A, Urbanová M, Baldrian J, Brus J, Šlouf M (2009) Structural and surface properties of novel polyurethane films. Mater Manuf Process 24:1214–1216
77. Prisacariu C, Scortanu E (2011) Influence of the type of chain extender and urethane group content on the mechanical properties of polyurethane elastomers with flexible hard segments. High Perform Polym 23:308–313